Journal of Directed Energy, **3**, Winter 2009, 276–288

Finite Element Analysis and Dynamic Simulation of Target Thermal Response to High-Energy Lasing

Christopher Larson, Clay Canning, Gunnar Tamm,* and John Hartke

United States Military Academy, West Point, New York 10996

High-energy laser (HEL) systems on the order of 100 kW are under development to neutralize stationary and mobile targets. Modeling the thermal response of the target will identify both requirements for the laser system and means to protect the target against such laser systems. Analytical solutions are limited, and computational solutions are accurate only if they consider boundary conditions and material properties varying with time, temperature, and location. A transient three-dimensional finite element solution has been developed that employs dynamic simulation techniques. Stationary and mobile targets are evaluated under loading by a continuous-wave laser with various beam profiles, with particular attention to mortar rounds in flight. Results from the target thermal model support complementary analyses of the 100-kW HEL system completed at the U.S. Military Academy.

KEYWORDS: Finite element, Heat transfer, High energy laser

Nomenclature

A	area, cm^2
c_p	specific heat, J/kg-K
d_z	length of element in z direction, cm
h	convection coefficient, W/m^2-K
k_{tc}	thermal conductivity, W/m-K
L	arc length of element, m
l	distance from laser to target, m
P_o	power at beam center, W
q	heat transfer rate, W
q''	heat flux, W/m^2
R	radial distance from beam central axis, cm
r_i	inner radius, cm
r_o	outer radius, cm

Received May 22, 2009; revision received December 28, 2009.
*Corresponding author; e-mail: Gunnar.Tamm@usma.edu.

T_{air}	air temperature, °C
$T_{(i,j,k)}$	temperature at element (i, j, k), °C
t	time, s
V	volume, m^3
w_o	beam waist, cm
w_z	spot size, cm
α	absorptivity
ε	emissivity
θ	laser incident angle, deg
θ_{BA}	beam half-angle, rad
λ	wavelength, μm
ρ	density, kg/m^3
σ	Stefan–Boltzmann constant, $W/m^2\text{-}K^4$
φ	circumferential direction

1. Introduction and Background

The impact of Counter-Rocket, Artillery, and Mortar (C-RAM) attacks during military operations can be reduced by using a high-energy laser (HEL) to destroy the incoming threat. This paper presents a thermal model for the interaction of the laser beam with the threat until it is neutralized. The model considers a common 81-mm mortar, here generalized to be a cylinder with a diameter of 81 mm. By modeling the laser–target interaction, HELs can be optimized for target lethality and for use on future battlefields. Countermeasures for a HEL employed in C-RAM operations are also identified.

The dynamic simulation software Powersim Studio is the platform onto which the model was built because of its ability to apply transient boundary conditions and varying material properties over finite time steps. The mortar is considered to be in flight with rotation and convection cooling. Advanced modeling for HELs is very difficult with an analytical model because of the nonlinear nature of the interaction. Numerical methods can handle changes in material properties and complex boundary layers as compared to analytical solutions.[4] Most models use self-built code and require large computing power. This dynamic simulation approach uses relatively little computing power but still engages full complexity. Ultimately the results can be validated experimentally and used to verify the results of other analytical and numerical work.

2. General Approach

The mortar was modeled as a cylinder with the laser striking the surface as a continuous wave, although pulsing can be readily incorporated. Dynamic simulation software uses finite time steps to discretize complex equations instead of taking the integral. This simplifies the analytical approach by changing the integral problem into a algebraic summation of thermal energy transfers:

$$\int_{t_1}^{t_2} q\,dt = \sum q\,\Delta t. \tag{1}$$

An advantage of finite element analysis (FEA) is the ability to include material properties and boundary conditions that vary in location, in time, and with temperature. Dynamic

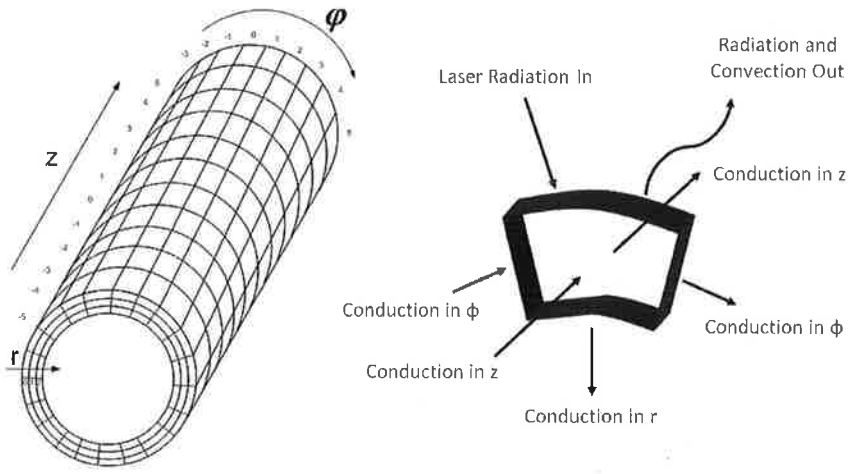

Fig. 1. Simplified finite element model of the target mortar.

simulation allows for feedback at each time interval to update the boundary conditions and material properties, as well as any other specified conditions such as material combustion or removal. The shape of the model is a cylinder with coordinates in the r, φ, z directions as shown in Fig. 1, along with the heat transfers for a surface element.

Heat transfer is driven by a temperature potential and limited by a thermal resistance. The thermal resistance due to radial conduction through a cylindrical shell is given in Eq. (2). Multiplication by the number of circumferential elements would give the radial conduction resistance of each element:

$$R_{\text{cond},r} = \frac{\ln(r_o/r_i)}{2\pi k_{tc} d_z}, \tag{2}$$

where r_o and r_i are the radii from the center of the cylinder to the midpoint of the interacting elements and d_z is the axial length of each element. The thermal conductivity, k_{tc}, is the average thermal conductivity of the two elements. The thermal conduction resistance in the circumferential direction is

$$R_{\text{cond},\varphi} = \frac{L}{k_{tc} A_\varphi}, \tag{3}$$

where L is the arc distance between the midpoints of the elements and A_ϕ is the elemental area perpendicular to heat transfer in the circumferential direction. The thermal conductivity, k_{tc}, is the average thermal conductivity of the two elements. The thermal conduction resistance in the axial direction is

$$R_{\text{cond},z} = \frac{d_z}{k_{tc} A_z}, \tag{4}$$

where d_z is the axial distance between the center point of the elements and A_z is the elemental area perpendicular to heat transfer in the axial direction. The thermal conductivity, k_{tc}, is the average thermal conductivity of the two elements. Thus, the conduction between elements in the radial (i-index), circumferential (j-index), and axial (k-index) directions, respectively,

are

$$q_r = \frac{T_{i,j,k} - T_{i+1,j,k}}{R_{\text{cond},r}}, \tag{5}$$

$$q_\varphi = \frac{T_{i,j,k} - T_{i,j+1,k}}{R_{\text{cond},\varphi}}, \tag{6}$$

$$q_z = \frac{T_{i,j,k} - T_{i,j,k+1}}{R_{\text{cond},z}}. \tag{7}$$

The thermal losses from the surface elements via convection and radiation are given as

$$q_{\text{convection}} = hA_s[T_{i,j,k} - T_{\text{air}}], \tag{8}$$

$$q_{\text{radiation}} = \sigma\varepsilon A_s[T^4_{i,j,k} - T^4_{\text{air}}], \tag{9}$$

where the convection heat transfer coefficient in Eq. (8) was estimated for flow over the cylindrical surface in the axial direction due to the mortar flight. The radiation gain from the laser is

$$q_{\text{laser}} = q''_{\text{laser}} A_s \alpha, \tag{10}$$

where q''_{laser} is the normal laser flux for the individual element, A_s is the surface area of the element, and α is the spectral absorptivity of the surface material. Conservation of energy for any element is given by Eq. (11) and accounts for the net heat flow through the six element faces balanced by the energy storage in the element:

$$\sum q = \rho V c_p \left(T_{t+\Delta t} - T_t\right). \tag{11}$$

Tabulated properties of specific heat, density, thermal conductivity, absorptivity, and emissivity were selected for different temperatures.[3,6,7] From these values the dynamic simulation software interpolated and extrapolated values at other temperatures.

The beam is modeled as a Gaussian profile according to the planar two-dimensional (2-D) Gaussian distribution:

$$q''_{\text{laser}} = \frac{P_o}{w_o^2}\left(\frac{w_o}{w_z}\right)^2 \frac{\pi}{4} e^{-2R^2/w_z^2}, \tag{12}$$

where R is the radial distance from the beam central axis and the diffraction-limited spot size and half-angle are given as

$$w_z = w_o + \ell\theta_{\text{BA}}, \tag{13}$$

$$\theta_{\text{BA}} = \frac{\lambda}{\pi w_o}. \tag{14}$$

To account for the distortion of the beam on the cylinder surface, the area of the cylinder was normalized into a planar 2-D surface. This allowed a more accurate model by accounting for the surface area of the cylinder that is normal to the laser radiation.

3. Results and Discussion

The primary goal of the simulation was to determine the kill time of heating the mortar until deflagration of the contained explosive. Several parametric effects stem from this model and are discussed as follows to emphasize the most significant factors.

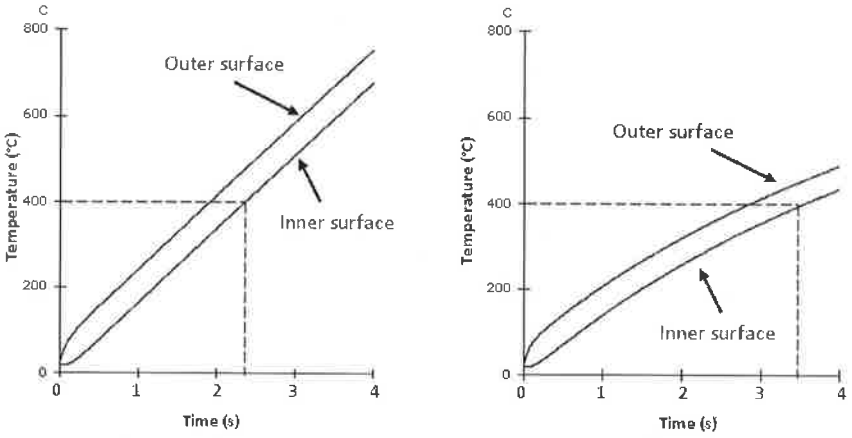

Fig. 2. Mortar temperature assuming constant (left) vs. variable (right) properties for uniform 1-D heating.

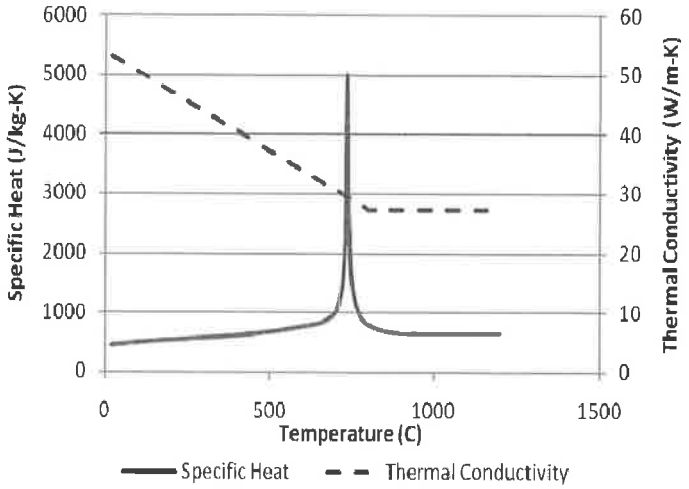

Fig. 3. Specific heat and thermal conductivity for carbon steel.

3.1. Variable properties

A one-dimensional (1-D) radial model readily illustrates the need to consider material properties that vary with temperature. The kill time is taken to be when the inside shell surface, and therefore the explosive, reaches 400°C while heated by a uniform radiant flux of 1,000 W/cm^2. As shown by the dashed lines in Fig. 2, the kill time is achieved in 2.3 s when assuming constant properties, but in 3.5 s with variable properties for the 1-cm-thick aluminum shell. A significant increase! This is caused by the decrease in the thermal conductivity and increase in the specific heat as the metal heats up. Both reduce the rate of thermal diffusion and thus extend the kill time. The surface absorptivity decreases with temperature as well, further reducing the impact of the laser beam by decreasing the absorbed radiation.

The specific heat and thermal conductivity of steel versus temperature can be seen in Fig. 3. Both of these relations are defined by stepwise functions.[1] A significant change

Table 1. Parameters of mortar targeted with Gaussian beam

Parameter	Value
Cylinder diameter	81 mm
Cylinder length	200 mm
Shell thickness	8.4 mm
Divisions in r direction	41
Divisions in φ direction	41
Divisions in z direction	31

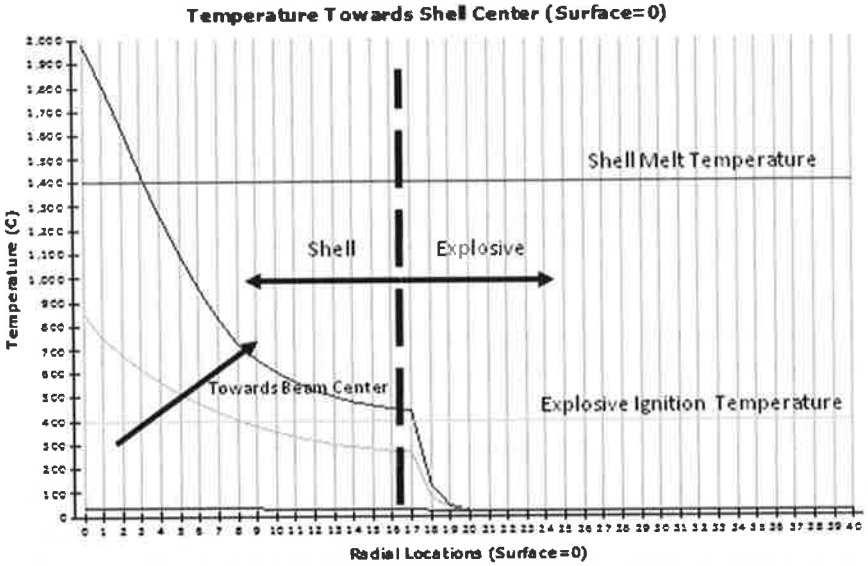

Fig. 4. Temperature at various radial locations after 3 s without rotation.

occurs for each property around 750°C, which can be attributed to the change of the material to the austenite phase. The induced change in the crystal structure from body-centered cubic to face-centered cubic absorbs most of the energy, which greatly increases the specific heat. Thermal conductivity reaches a bottom plateau at this temperature. During this transition, the sensible temperature increase would be greatly subdued, further increasing the kill time to heat the explosive.

Computational modeling allows for multiple material layers to be present, with the mortar parameters given in Table 1. Figure 4 shows the temperature variation through both the aluminum shell and RDX (cyclotrimethylenetrinitramine) explosive at a given time. Note the sudden drop in temperature across the explosive due to the low thermal conductivity, with properties given in Table 2.[2,5] Analytical solutions would model the explosive as an insulated boundary for the shell, but this would incorrectly lead to a 10% faster kill time for the inside of the shell to reach 400°C. Note that the aluminum shell outer surface would reach 1,400°C and begin to melt at 1.55 s, and the explosive would ignite after 2.77 s in this

Table 2. Properties of RDX explosive[2,5]

Parameter	Value
Density	1,800 kg/m^3
Specific heat	2,100 J/kg-K
Thermal conductivity	0.3 W/m-K

Table 3. Gaussian beam properties

Parameter	Value
Power	100 kW
Wavelength	1,064 μm
Beam waist	3 cm
Spot size	6.39 cm
Distance to target	3,000 m
Shell melt temperature	1,400°C
Explosive ignition temperature	400°C

model without rotation. The melted region would be 2 mm deep with a melted diameter of 26 mm. The Gaussian beam parameters are given in Table 3.

3.2. Surface heat transfer

The convection and radiation loss is insignificant in the region heated by the laser. This allows for the convection and radiation losses to be approximated with only minimal error. Only during rotation, when a surface element rotates out of the laser sight, does convection and radiation loss become significant. Figures 5 and 6 compare the absorbed radiation and heat losses from the same surface element on the cylinder. The absorbed radiation in Fig. 5 decreases as the absorptivity decreases with increased temperature. The heat losses are negligible in comparison to the laser gain but increase with time as the surface temperature increases. Radiation losses increase at a faster rate than the convective cooling as radiation is proportional to the fourth power of temperature.

3.3. Mortar rotation

Mortars are fired from a smooth bore and are fin stabilized, but tolerances in manufacturing can produce spin rates of 1–4 Hz. This rotation will translate into a periodic heating as sections of the surface rotate into and out of the laser beam. Figure 7 shows the surface temperature and an interior temperature for a rotation of 1 Hz, for which the explosive will reach 400°C and deflagrate after 5.5 s. The surface element heats up while the laser is incident upon it but then cools via convection and radiation to the surroundings, as well as conduction into the adjacent elements. There is considerable cooling when the target is not in contact with the laser beam. The large amplitude in temperatures at the surface is

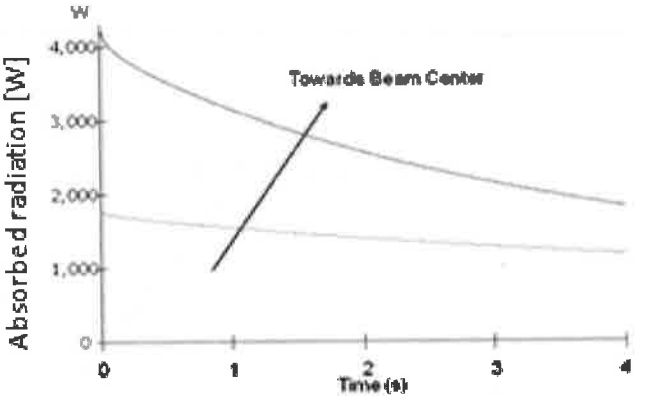

Fig. 5. Surface radiation input to an element at the beam center.

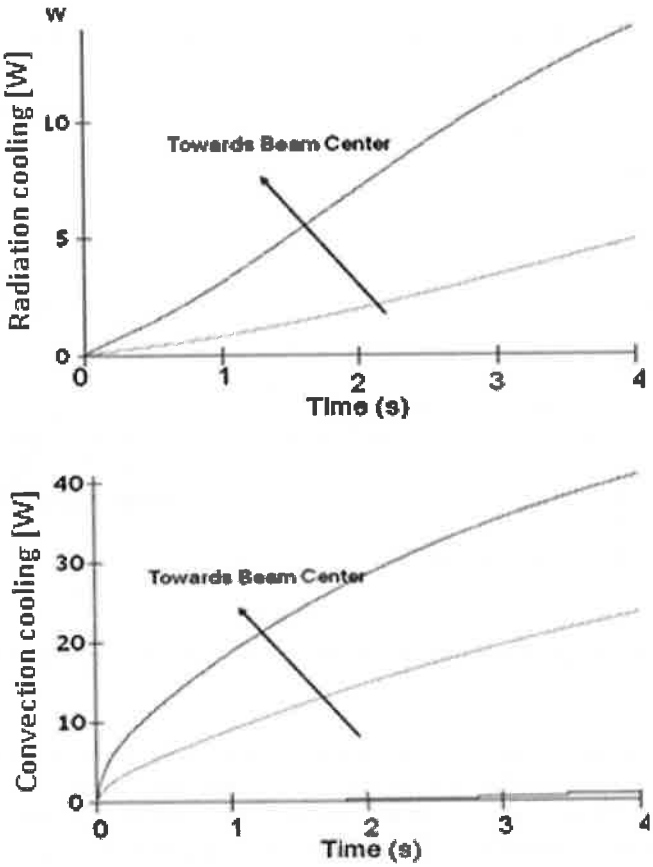

Fig. 6. Surface convection and radiation losses from an element at the beam center.

minimized significantly at the inner elements shown, where the deflagration would occur, and a phase lag is present during the periodic heating.

Figure 8 shows the effect of a faster rotation of 10 Hz, in which the explosive will deflagrate after 5.7 s. Kill times for various rotational rates are summarized in

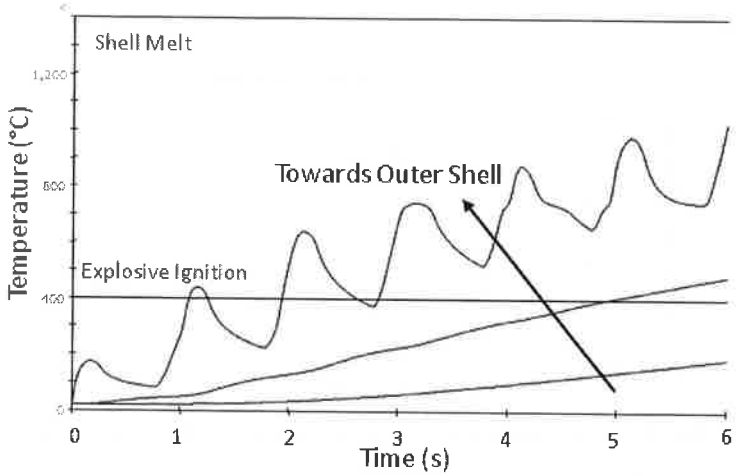

Fig. 7. Temperature at various locations of a rotating round at 1 Hz.

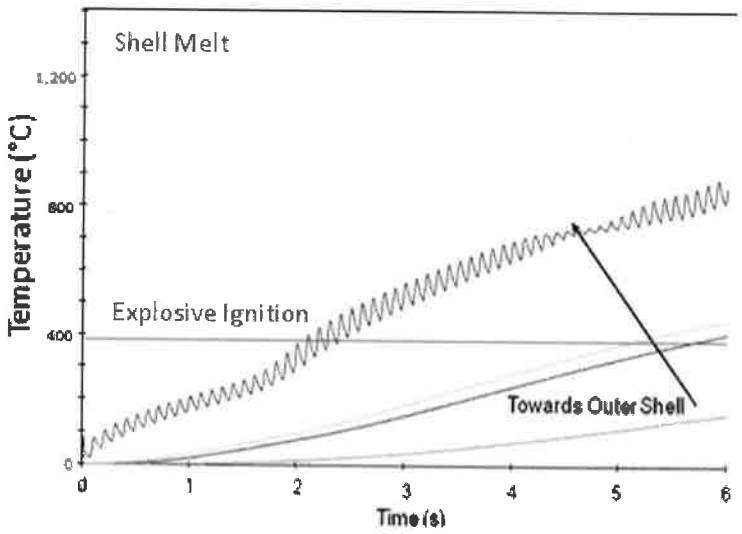

Fig. 8. Temperature at various locations of a rotating round at 10 Hz.

Table 4. A mortar that rotates will take longer to destroy than one that does not rotate, as the target area will be able to cool once on the dark side of the rotation. For faster rotations the temperature swells will become negligible and the kill time will not vary noticeably with the rotational rate. None of the mortar exteriors that are rotating above 1 Hz reached the melting temperature, as occurred without rotation.

3.4. Appropriate mesh size

To assess the necessary mesh size, the simulation was repeated at various mesh sizes to compare kill time results. A large mesh takes a significantly longer time to run than a small

Table 4. Explosive ignition time for various frequencies

Frequency (Hz)	Kill time (s)
0	2.77
1	5.47
10	5.72
100	6.02

Table 5. Effect of mesh size on neutralization time

Parameter	Small mesh	Medium mesh	Large mesh
No. of elements	7,497	52,111	169,371
Explosive ignition, s	2.67	2.77	2.77
Surface melt, s	1.77	1.55	1.55

Table 6. Atmospheric and beam parameters

Parameter	Value
Aerosol	Desert
Atmosphere	Desert winter
Distance to target	3,000 m
Beam quality	2
Beam waist	3 cm
Spot size	75.4 cm
Transmittance	0.685

mesh. As shown in Table 5, the large mesh had more than twice as many elements as the medium mesh with no difference in the results. This was a significant validation because it allowed the model to be utilized with a smaller mesh that uses less computing power and compiles in a much shorter time. On the other end, use of a too-small mesh can lead to errors.

3.5. Effects of desert atmosphere

If a HEL system is employed in a current theater of operations, it would be in a desert environment. Beam properties for the base model in a desert application are shown in Table 6.

The large spot size is the result of significant beam blooming and drastically affects the HEL effectiveness. This effect would be less pronounced the closer the laser is to the target. The temperatures of the model at the end of a 4-s simulation are shown in Table 7, where

Table 7. Temperature at 4 s with significant thermal bloom

Power (kW)	Outer shell temp (°C)	Inner shell temp (°C)
115	32.1	28.8
100	30.5	27.7
80	28.4	26.2

Table 8. Diffraction-limited case with 100-kW beam power

Wavelength (μm)	Spot size (cm)	Explosive ignition time (s)	Shell melt time (s)
1.064	6.4	2.77	1.55
1.315	7.2	1.60	2.18
1.625	8.2	1.97	3.49
2.141	9.8	2.73	>4

the starting temperature was taken to be 20°C. Given the significant thermal bloom, clearly the laser would be ineffective until the mortar is closer to the laser origin.

3.6. Effects of beam wavelength

Higher wavelengths increase the angle of diffraction, which results in a larger spot size on target. An increase in spot size greatly reduces the intensity of the laser, thus increasing the kill time as shown in Table 8.

By comparing the increases in power vs. spot size for a HEL, it is much more important to have a high beam quality than high power rating. A large beam quality greatly decreases the effectiveness of the laser.

3.7. Defeating HELs in C-RAM applications

A method to defeat HEL systems would be to place a thin insulating material between the shell and the explosive to delay the deflagration of the high explosive. This would force the HEL system to stay on target longer to neutralize the target. If the insulating layer was employed on a rotating round, then the time to melt the round would increase significantly, and the kill mechanism would involve melting through the shell. Another countermeasure would be to encase the mortar round in a shell with poor conductivity and poor absorptivity. This goes beyond simply painting the mortar with a reflecting coating, which is ineffective as the paint quickly burns off or produces a high-absorptivity char. These countermeasures will be explored in further models.

4. Conclusions

A thermal model for the interaction of a 1,000-W/cm^2 laser with a mortar has been employed to estimate its kill time. The use of variable properties, a layered three-dimensional

geometry, and transient boundary conditions was supported by using a finite element approach powered by the dynamic simulation platform Studio. Depending on the operating conditions, the kill time ranged from 2 to 6 s, which agrees with experimentally available data. Specific findings include the following:

- Modeling with variable properties instead of constant properties increases the kill time by 50%.
- The absorbed radiation is at least one order of magnitude greater than the thermal losses via radiation and convection.
- A mortar that does not rotate has a kill time of 2.8 s, whereas a typical rotation of 1–4 Hz requires a kill time of 5.5 s.

5. Acknowledgments

We would like to thank the High Energy Laser Joint Technology Office (HEL JTO) for funding our research project and the director, Mark Niece, for his insight. Gabriel Costa of the Department of Mathematical Sciences at West Point provided mathematical expertise in calculating the distortion of the beam striking the surface at a skew angle. Peeter Nielander provided administrative support during the editing process. The views expressed herein are those of the authors and do not purport to reflect the position of the United States Military Academy, the Department of the Army, or the Department of Defense.

References

[1]Bailey, C. "Carbon Steel Thermal Properties," One Stop Shop in Structural Fire Engineering, University of Manchester, http://www.mace.manchester.ac.uk/project/research/structures/strucfire/materialInFire/Steel/HotRolledCarbonSteel/thermalProperties.htm, retrieved December 8, 2007.

[2]Beyer, J.C., J.K Arima, and D.W. Johnson, "Enemy Ordance Materiel," in *Wound Ballistics*, edited by J.C. Beyer, Medical Department, U.S. Army, http://history.amedd.army.mil/booksdocs/wwii/woundblstcs/chapter1.2.htm, retrieved January 20, 2009.

[3]Incropera, F.P., D.P. Dewitt, T.L. Bergman, and A.S. Lavine, *Fundamentals of Heat and Mass Transfer* (6th ed.), Wiley, New York (2007).

[4]LaMar, C., "Applications of Analytical Solutions for the Laser Heating of Materials," Proceedings of the 2008 Directed Energy Systems Symposium, U.S. Army Space and Missile Defense Command, Huntsville, AL (2008).

[5]Rubenchik, A.M., Propellants, Explosives Pyrotechnics **32**(4), 269 (2007).

[6]Rudder, R.R., "A Summary of High-Energy Laser Lethality Testing on Aluminum," Technical Report AFRL-DE-PS-TR-2007-1119, Air Force Research Laboratory, Kirtland Air Force Base, 19 June 2007.

[7]Walters, C.T., "A Summary of High-Energy Laser Lethality Testing on Steels," Technical Report AFRL-DE-PS-TR-2007-1118, Air Force Research Laboratory, Kirtland Air Force Base, 19 June 2007.

The Authors

Mr. Clay Canning received his undergraduate degree in mechanical engineering from the U.S. Military Academy in 2009 and was commissioned as a second lieutenant upon graduation to continue serving on active duty. This work was performed as an independent study while he was a cadet.

Dr. John Hartke is an Academy Professor in the Department of Physics and Lieutenant Colonel in the U.S. Army. He serves as the project coordinator for West Point's high-energy laser effort through his leadership in the Photonics Research Center.

Mr. Christopher Larson received his undergraduate degree in mechanical engineering from the U.S. Military Academy in 2009 and was commissioned as a second lieutenant upon graduation to continue serving on active duty. This work was performed as an independent study while he was a cadet.

Dr. Gunnar Tamm is an Associate Professor in the Department of Civil and Mechanical Engineering and served as the project advisor for the heat transfer team in this multidisciplinary effort at West Point to model high-energy laser systems.

Technical Scope of Submissions

The Journal of Directed Energy solicits and publishes papers in all aspects of DE, and with particular emphasis on the engineering issues of the discipline, including but not limited to the following:

DE System Design
High Energy Lasers
Laser Optics
Acquisition, Tracking, and Pointing
Propagation Effects
High Power Microwave Sources
Pulsed Electromagnetics
Antenna Systems
Vulnerability Assessment
DE Modeling and Simulation
Human Factors
Self Protection Issues
Test and Evaluation

Instructions for authors:

Manuscripts should be submitted electronically as Microsoft Word or PDF documents according to the requirements found at www.deps.org/DEPSpages/DEjournal.html. Include full information (*including address, phone, fax, and e-mail*) for corresponding author to receive proofs. Supply names and contact information of five suggested reviewers, although the editors reserve the right to choose their own reviewers independent of the list supplied. Queries to the author will be typeset in the proof, and proofs will be e-mailed to authors as pdf files, or mailed if e-mail not available. Authors will relay corrections to compositor by e-mail, fax, or mail.

Authors must submit the DEPS copyright form with the paper so that the editor may accept the paper for review, along with written assurance that appropriate security clearance has been obtained. It is the author's responsibility also to provide written assurance that the paper has not been published, nor under consideration, elsewhere and they are willing to make revisions in the paper, if necessary.

Papers should be in American rather than British spelling, using the serial comma, with the use of standard abbreviations for units. (g not gm for gram, for example) Metric or dual systems of units (metric and English) are allowed. Authors should spell out numbers through ten except when used with a unit. Numbers should use the comma in numerals of four or more digits. Papers may use "et al." in the text but the authors need to include all names in the reference list. Acronyms (except for designations) would have to be spelled out at first use and would be allowed even if not used again. Authors should follow standards for setting math given in the book Mathematics in Type.

Papers must include a brief (100 to 200 word) abstract that explains the object of the investigation and the major results. For indexing purposes three to five keywords must be indicated. A nomenclature section must follow the abstract in which all symbols are identified. An introduction explaining previous work and the contribution provided by the submitted paper follows the nomenclature section. A section clearly explaining the conclusions that may be drawn from the results and their significance is the last section of the text, followed by the list of references, tables in numerical order, and then the figures in numerical order. Papers should be no more than 32 double-spaced, 12-point font, pages long in total.

References must be easily accessible public documents and are to be placed at the end of the paper in alphabetical order by first author's last name. References, figures, and tables have to be mentioned in the text. Tables must have a double rule at the top and bottom of the table with a single rule under column headings, with any footnotes placed under the bottom double rule. Illustrations must be clear and sharp with lettering large enough to be easily legible. Each figure must be a separate page and the captions should be listed in numerical order on a separate page. Table and figures can be mentioned out of order parenthetically (that is, a figure that is discussed later could be referred to earlier) Reference callouts in figures or tables are adequate; it's not necessary that the references also be mentioned in the text. Photographs must be glossy prints. Footnotes to the text are acceptable.

Color illustrations or photographs will be published if the editors deem it necessary for clarity. Use of color involves substantial expense and the author's employer must pay the full incremental cost of color publication (minimum of $1000 for production costs, plus $75 per figure for color separations; actual costs may vary).

The JDE will not accept papers for publication that do not adequately address the accuracy of the results, whether computational or experimental.